

Deliquescence of small particles

Lynn M. Russell

Department of Chemical Engineering, Princeton University, Princeton, New Jersey 08544

Yi Ming

Department of Civil and Environmental Engineering, Princeton University, Princeton, New Jersey 08544

(Received 2 July 2001; accepted 2 October 2001)

The deliquescence of particles smaller than 100 nm in diameter from crystalline form to liquid droplets involves both solvation effects and surface energies. Here we study this phenomenon for the case of salt particles of initial dry diameters from 8 to 100 nm that are exposed to humid conditions from 45 to 95% relative humidity. With a simple thermodynamic equilibrium model for three soluble species (sodium chloride, ammonium sulfate, and a soluble organic compound), we show that the role of surface tension is to increase the relative humidity at which particles will deliquesce. For example, 15 nm dry diameter sodium chloride particles deliquesce at 83%, an 8% increase over the 75% deliquescence relative humidity for supermicron droplets and bulk solution. Many soluble species in air above 45% relative humidity are wetted with multiple layers of water molecules such that the relevant interface is that between the partially dissolved salt crystal and a saturated salt solution rather than between the dry crystal and air. Since surface tensions for this solid/liquid interface are not well known, a range of values have been used from the literature, yielding consistent results. While the existence of unstable equilibria during deliquescence of the system precludes complete experimental verification of the predicted behavior with measurements, a recent experiment suggests indirect agreement with the change in predicted deliquescence relative humidity. © 2002 American Institute of Physics. [DOI: [10.1063/1.1420727]]

I. INTRODUCTION

Particles of sizes between 8 and 100 nm in diameter are ubiquitous in the lower troposphere. The way in which these particles take up water is critical in determining their role in forming haze and clouds as well as in serving as sites for heterogeneous chemical reactions. This hygroscopic growth of particles has important consequences for the predicted atmospheric radiative transfer of aerosols and their effect on climate.¹ To date the hygroscopic behavior of particles has been studied with both experimental measurements and numerical models.

For inorganic salts and a few organic species, careful measurements have been undertaken to predict the relative humidity at which water uptake is initiated (deliquescence) and the amount of water that particles of different compositions will accrete as the relative humidity continues to rise after this deliquescence point.²⁻⁵ In all but one case,⁴ these studies have focused on particles with initial dry diameters of 100 nm or greater. Measuring smaller particles has been precluded by experimental limitations on particle detection and trace contamination.

Physical descriptions of the deliquescence process have been provided by a series of standard texts for particles that are sufficiently large that the surface tension of the liquid/vapor interface is negligible.⁶⁻⁸ More recently Mirabel *et al.*⁹ posed the question of small particle deliquescence for a generic crystal forming an ideal solution and predicted the relative humidity for prompt (or uncoated) deliquescence and its dependence on particle size. While we describe a similar physical system, the nonideal aspects of the problem for the

real species we have studied change the predicted behavior such that our coated model predicts an inverse dependence of deliquescence relative humidity on particle size in contradiction to the proportional dependence predicted by the idealized, uncoated deliquescence model. The systems described by the coated and uncoated models are illustrated schematically in Fig. 1.

II. DELIQUESCENT OF WETTED PARTICLES

Mirabel *et al.*⁹ proposed a scenario for prompt deliquescence of particles that identified the relative humidity predicted for the transition from a dry crystal particle to a dissolved salt droplet. This approach relies on the particle being dry at the point of deliquescence. While this assumption may hold for some salts, several studies have shown that water adsorbs approximately two monolayers of water on the surface of crystalline sodium chloride before the relative humidity reaches 45%, with four layers accumulating at 70%.¹⁰⁻¹⁴ In fact, recent work has suggested anomalously high water amounts below the deliquescence relative humidity for particles smaller than 400 nm.¹⁵ Hence, for deliquescence points at higher relative humidities, the Gibbs free energy of the phase change should be predicted by difference of the dissolved particle compared to the wetted particle rather than to the dry crystal.¹⁶

The difficulty of this approach is that it requires describing the free energy of the adsorbed water layer and its interface, since the surface energy of a thin adsorbed layer on a crystal of unknown geometry is poorly constrained. However, Ewing and co-workers have shown that the properties

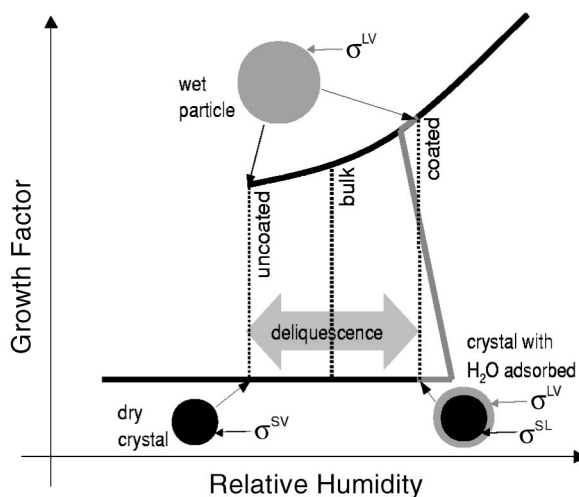


FIG. 1. Schematic diagram of deliquescence of a salt crystal with two models: the coated model assumes that prior to deliquescence multiple water layers will be adsorbed on the crystal surface whereas the uncoated model assumes the vapor interfaces with the solid crystal. The difference for dry particles smaller than 100 nm dry diameter is that, when compared with the deliquescence of a bulk phase, the uncoated model predicts lower deliquescence relative humidities and the coated model predicts higher deliquescence relative humidities. In the diagram, the solid lines represent dry (thin) and wet (thick) states and the dotted lines show deliquescence. The gray line shows unstable equilibria for partially wet states resulting from the role of surface tension in the coated model.

of the adsorbed layer in humid conditions are indistinguishable from an aqueous salt solution, so that the use of bulk liquid surface properties is appropriate.^{17–20} For the case of a powder or a partially dissolved crystal, it is also appropriate to assume that the crystal or any remaining undissolved fraction is spherical.^{6,21} To assess the sensitivity to this assumption, we also consider the case of a cubic crystal in Sec. V.

The second assumption is that the surface energy of the interior and exterior interfaces of this spherical shell of water can be described by bulk surface tension. Several authors have noted the inadequacy of bulk surface tension for finite-molecule systems such as nucleating clusters, and the same criticism applies to the four layers of adsorbed water in our current usage.^{6,22,23} The point at which deliquescence occurs is dependent on the adsorbed liquid amount and the surface energy of that thin layer. Bulk surface tension values are the best estimate currently available for this purpose, and recent work experimentally verifying the Kelvin effect for cyclohexane bubbles as small as 4 nm suggests that they may be appropriate.²⁴ To quantify the potential impact of variation of surface tension for finite-molecule situations,²² we have studied the sensitivity of this prediction to size-dependent surface tension using a simple Tolman length model in Sec. V.⁶

The coated model is described by the following equation for the free energy G of the aerosol system at constant temperature and pressure (including solid S representing crystalline NaCl, liquid L consisting of water and dissolved NaCl, and vapor V containing water and air):

$$G_{\text{coated}} = \mu_{\text{coated}}^S n_{\text{coated}}^S + \mu_{\text{coated}}^L n_{\text{coated}}^L + \mu_{\text{coated}}^V n_{\text{coated}}^V + \sigma^{\text{SL}} a_{\text{coated}}^{\text{SL}} + \sigma^{\text{LV}} a_{\text{coated}}^{\text{LV}}, \quad (1)$$

where μ^S , μ^L , and μ^V are the chemical potentials of the solid, liquid and vapor phases (assuming only one phase of each type), respectively, and n^S , n^L , and n^V are the numbers of moles of the solid, liquid, and vapor phases, respectively.⁹ Note that μ^L is a function of the mole fraction of sodium chloride dissolved, x_{NaCl} . The free energies of the solid/liquid (SL) and liquid/vapor (LV) interfaces are given by the products of their surface tensions σ^{SL} and σ^{LV} and the interfacial areas a^{SL} and a^{LV} . The subscript coated is used to indicate the dry phase description used in each of the two models illustrated in Fig. 1. The particle before deliquescence in the uncoated model has no liquid phase and is simply represented by

$$G_{\text{uncoated}} = \mu_{\text{uncoated}}^S n_{\text{uncoated}}^S + \mu_{\text{uncoated}}^V n_{\text{uncoated}}^V + \sigma^{\text{SV}} a_{\text{uncoated}}^{\text{SV}}. \quad (2)$$

Once the crystal phase has disappeared in either model, there is only a liquid phase and a vapor phase such that the free energy simplifies for the wet droplet to the following form

$$G_{\text{wet}} = \mu_{\text{wet}}^L n_{\text{wet}}^L + \mu_{\text{wet}}^V n_{\text{wet}}^V + \sigma^{\text{LV}} a_{\text{wet}}^{\text{LV}}. \quad (3)$$

In order to compare free energies of these wet and dry (coated and uncoated) particles, the free energy is corrected to standard reference states, such that

$$\Delta G_{\text{coated}} \equiv G_{\text{coated}} - G^0. \quad (4)$$

Note that the reference state G^0 is the same for both wet and dry forms in both the coated and uncoated models since it is dependent only on the total amounts of NaCl and H_2O in all phases of the system:

$$G^0 \equiv G_{\text{wet}}^0 \equiv G_{\text{coated}}^0 \equiv G_{\text{uncoated}}^0. \quad (5)$$

The change in free energy due to deliquescence is then described by the difference between the wet droplet and the dry particle, so that for the coated particle model

$$\begin{aligned} \Delta G_{\text{coated}}^{\text{deliq}} &\equiv \Delta G_{\text{wet}} - \Delta G_{\text{coated}} \\ &= \mu_{\text{wet}}^L n_{\text{wet}}^L + \mu_{\text{wet}}^V n_{\text{wet}}^V + \sigma^{\text{LV}} a_{\text{wet}}^{\text{LV}} \\ &\quad - \mu_{\text{coated}}^S n_{\text{coated}}^S - \mu_{\text{coated}}^L n_{\text{coated}}^L - \mu_{\text{coated}}^V n_{\text{coated}}^V \\ &\quad - \sigma^{\text{SL}} a_{\text{coated}}^{\text{SL}} - \sigma^{\text{LV}} a_{\text{coated}}^{\text{LV}}, \end{aligned} \quad (6)$$

in which the reference states have cancelled out. For the uncoated model, the free energy change at deliquescence is dependent on the solid/vapor interfacial energy rather than the solid/liquid energies. It can be written as

$$\begin{aligned} \Delta G_{\text{uncoated}}^{\text{deliq}} &\equiv \Delta G_{\text{wet}} - \Delta G_{\text{uncoated}} \\ &= \mu_{\text{wet}}^L n_{\text{wet}}^L + \mu_{\text{wet}}^V n_{\text{wet}}^V \\ &\quad + \sigma^{\text{LV}} a_{\text{wet}}^{\text{LV}} - \mu_{\text{uncoated}}^S n_{\text{uncoated}}^S \\ &\quad - \mu_{\text{uncoated}}^V n_{\text{uncoated}}^V - \sigma^{\text{SV}} a_{\text{uncoated}}^{\text{SV}}. \end{aligned} \quad (7)$$

Deliquescence occurs when the free energy of the completely wet droplet (G_{wet}) equals that of the water-coated crystal (G_{coated}), which can be expressed as the difference in those free energies ΔG^{deliq} for either the coated or uncoated model equaling zero,

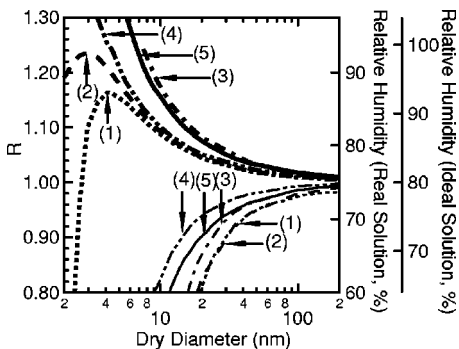


FIG. 2. Predicted deliquescence relative humidity ratio R as a function of dry particle size. The thick and thin curves correspond to $\sigma^{SV}=100$ and $\sigma^{SV}=270 \text{ mN m}^{-1}$, respectively. The lines represent (1) uncoated model (Ref. 9) with ideal solution, constant partial molar volume \bar{v} , and $\sigma^{LV}=70 \text{ mN m}^{-1}$ (dotted line), (2) uncoated model (Ref. 9) with ideal solution, measured \bar{v} , and $\sigma^{LV}=70 \text{ mN m}^{-1}$ (dashed line), (3) uncoated model (Ref. 9) with ideal solution, measured \bar{v} , and $\sigma^{LV}=83 \text{ mN m}^{-1}$ (dashed-dotted line), (4) uncoated model (Ref. 9) with real solution, constant \bar{v} , and $\sigma^{LV}=70 \text{ mN m}^{-1}$ (dashed-dotted-dotted line), and (5) coated particle model with real solution, measured \bar{v} , and $\sigma^{LV}=83 \text{ mN m}^{-1}$ (solid line) (this work).

$$\Delta G_{\text{coated}}^{\text{deliq}} = 0 \tag{8}$$

and

$$\Delta G_{\text{uncoated}}^{\text{deliq}} = 0. \tag{9}$$

The equilibria found from this equation are not all stable points, so we examine in Sec. IV the question of which predicted equilibrium point is stable for each specified temperature, pressure, and relative humidity. After dissolution of the solid species, both Eqs. (8) and (9) reduce to the familiar Kelvin equation

$$RH \equiv 100 \times \frac{p_w(D_p)}{p_w^o} = 100 \times x_w \gamma_w \exp\left(\frac{4M_w \sigma^{LV}}{RT \rho_w D_p}\right), \tag{10}$$

where RH is the relative humidity of water vapor, p_w is the water vapor pressure in equilibrium with a particle of diameter D_p , p_w^o is the saturation vapor pressure of water, σ^{LV} is the surface tension at the liquid/vapor interface, x_w and γ_w are the mole fraction and activity coefficient of water in the aerosol phase, respectively, and M_w and ρ_w are the molecular weight and density of water at temperature T .

III. COMPARISON OF DELIQUESCENT MODELS

To illustrate the behavior of the coated model to the idealized, uncoated model, Fig. 2 shows the dependence of the predicted deliquescence relative humidity ratio R on particle size, where

$$R \equiv \frac{DRH(D_p)}{DRH(D_p^\infty)} \tag{11}$$

is defined as in Mirabel *et al.*⁹ DRH is the deliquescence relative humidity, or the relative humidity at which the wet droplet is stable with respect to the dry (coated or uncoated) salt crystal, D_p is the dry particle diameter, and D_p^∞ is a diameter sufficiently large that the particle behavior is negligibly different from a bulk solution (i.e., typically greater

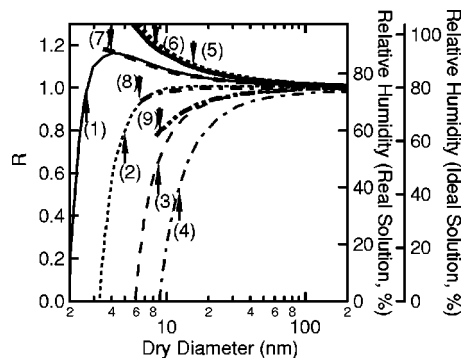


FIG. 3. Comparison of deliquescence relative humidity ratio R predicted with dry and coated models. For the uncoated particle model (thin lines), Mirabel *et al.* (Ref. 9) considered the case of $\sigma^{LV}=70 \text{ mN m}^{-1}$ and the following range of solid/vapor surface tension values: (1) $\sigma^{SV}=100 \text{ mN m}^{-1}$ (thin solid line), (2) $\sigma^{SV}=112 \text{ mN m}^{-1}$ (thin dotted line), (3) $\sigma^{SV}=200 \text{ mN m}^{-1}$ (thin dashed line), and (4) $\sigma^{SV}=270 \text{ mN m}^{-1}$ (thin dashed-dotted line). For the coated model proposed in this work (thick lines), $\sigma^{LV}=83 \text{ mN m}^{-1}$ and the following values of solid/liquid surface tension have been studied: (5) $\sigma^{SL}=17 \text{ mN m}^{-1}$ (thick dotted line), (6) $\sigma^{SL}=29 \text{ mN m}^{-1}$ (thick solid line), (7) $\sigma^{SL}=67 \text{ mN m}^{-1}$ (thick dashed line), (8) $\sigma^{SL}=117 \text{ mN m}^{-1}$ (thick dashed-dotted line), and (9) $\sigma^{SL}=187 \text{ mN m}^{-1}$ (thick dashed-dotted-dotted line).

than 100 nm diameter for the species studied in this work). The coated model predicts higher values of DRH and R than the idealized uncoated model for all values of surface tension.⁹

Since a sodium chloride solution is highly nonideal, the ideal solution assumption and estimated solubility of 0.20 (mole fraction) proposed previously⁹ changes $DRH(D_p^\infty)$ from 75 to 80%, but this assumption shows only a small change in the value of the R in Fig. 2 since the ratio normalizes DRH to remove this discrepancy. Nonetheless the actual DRH changes significantly as is illustrated by the comparison of R values to the equivalent real-solution DRH and ideal-solution DRH in the right-hand axes of Fig. 2.

The assumption that a particle will be coated prior to deliquescence when it is in equilibrium at a relative humidity of 70% accounts for the majority of the increase in R . The uncoated model compares the change in free energy from dry crystal to droplet, so that the only interface in the undeliquesced particle is the solid/vapor interface. This interfacial energy is characterized by the crystal surface tension which has been measured to be 213 mN m^{-1} ,⁷ although the uncertainty is large as other measured values range from 100 to 270 mN m^{-1} . For the coated model, the dry (or “undeliquesced”) particle has two interfaces, the solid/liquid and liquid/vapor interfaces with surface tensions $\sigma^{SL}=29 \pm 20 \text{ mN m}^{-1}$ and $\sigma^{LV}=83 \pm 2 \text{ mN m}^{-1}$.^{7,25,26} The coated model then has significantly higher R , since the liquid/vapor interfacial pressure partially counteracts the solid/liquid interfacial pressure and since the solid/liquid interfacial tension is much lower than that of a solid/vapor interface.¹⁶

Figure 3 shows the impact of surface tension on the predicted deliquescence relative humidity ratio R . Section IV discusses the range of probable values for these surface tensions in order to summarize the behavior of each model given current surface tension measurements.^{7,25,26} The isopleths show the boundary between $R > 1$ and $R < 1$ for three

sizes of dry particle. The shaded areas illustrate the range of recent reported measurements for both models. While there is some uncertainty in these values, with current measurements the coated model predicts $R > 1$ and the uncoated model $R < 1$ for respective surface tension ranges appropriate for NaCl. The robustness of the coated results over a large range of surface tensions mean that the use of bulk σ^{SL} may not introduce a significant error from the size-dependent behavior of small, thin surfaces, so that the results predicted here will be retained qualitatively once the dependence of surface tension on clusters of small sizes can be measured. A lower bound for this model is 8 nm dry diameter since smaller particles do not deliquesce below saturation with the coated model.

Modeling the thin liquid layer as bulk liquid interfaces to the solid and vapor phases simplifies the solid/liquid interface that might actually be characterized by a more complex interfacial region of quasi-solid, quasi-liquid molecules that have properties dissimilar from bulk liquid and solid phases. For particles greater than 15 nm dry diameter, this liquid layer will be sufficiently thick for growth factors greater than 1.2 (corresponding to approximately a 20-water-molecule-thick layer) that the bulk properties are appropriate. Section V investigates the role of this assumption by evaluating the hygroscopic growth with a Tolman length dependence of surface tension on size.⁶ However, recent work suggests that even three to four layers of adsorbed water will exhibit properties of bulk water, suggesting that the bulk interface behavior may be appropriate.^{17–20}

Incorporating concentration-varying density in the calculation also increases the predicted deliquescence relative humidity.² This approach accounts for a 4% increase over the prediction assuming constant density. The effect of this assumption is illustrated in Fig. 2.

An additional simplifying assumption in the model is that the crystal, its coating, and the droplet are all spherical. (This assumption is employed in both the coated and uncoated models.) For the coated model, the determining factor in the calculation is the shape of the coated particle. Some crystal species including ammonium sulfate are nearly spherical. Typical atmospheric particles such as mixtures of inorganic salts with organic impurities are likely to be nearly amorphous in the dry state rather than forming crystals, and such amorphous solids can be appropriately considered spherical. Nearest-neighbor and surface-defect considerations suggest that even those particles that tend to be cuboidal when dry will have their corners rounded by the presence of adsorbed water layers.²⁷ The cubic shape does not change the qualitative behavior of increasing DRH as particle size decreases shown in Fig. 2, but to bound the uncertainty of DRH due to shape, the growth of a cubic crystal is quantified in Sec. V.

IV. HYGROSCOPIC GROWTH AND STABILITY

The equilibria predicted by Eqs. (8) and (9) determined for the coated and uncoated models may be stable, unstable or metastable under humid atmospheric conditions. To assess the stability of the predicted equilibria, we evaluate

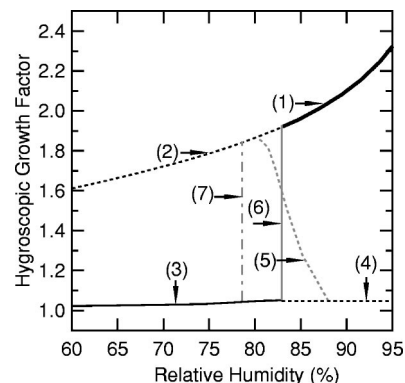


FIG. 4. Predicted hygroscopic growth factor of 15 nm dry diameter NaCl particles for coated and uncoated deliquescence models. The graph shows the coated particle model for (1) stable equilibria for the wet particle (thick solid line), (2) metastable equilibria for the wet particle (dotted line), (3) stable equilibria for the dry particle (thin solid black line), (4) unstable equilibria for the dry particle (dotted line), (5) unstable equilibria for partially wet particles (gray dotted line), and (6) deliquescence (gray solid line). For the uncoated particle model, the only difference in predicted equilibria is (7) deliquescence at a lower relative humidity (dashed-dotted gray line).

$$\left. \frac{\partial^2 G_{\text{coated}}}{\partial x_{\text{NaCl}}^2} \right|_{\text{deliq}} \approx \frac{\partial \Delta G_{\text{coated}}^{\text{deliq}}}{\partial x_{\text{NaCl}}} \quad (12)$$

This second derivative of the free energy describes the change of the slope of the free energy and represents a minimum in free energy internal to the parameter boundaries if and only if

$$\left. \frac{\partial^2 G_{\text{coated}}}{\partial x_{\text{NaCl}}^2} \right|_{\text{deliq}} > 0. \quad (13)$$

Such a minimum will form a stable equilibrium, as small perturbations will return to this value. Unstable equilibria are characterized by

$$\left. \frac{\partial^2 G_{\text{coated}}}{\partial x_{\text{NaCl}}^2} \right|_{\text{deliq}} < 0, \quad (14)$$

where x_{NaCl} is the mole fraction of sodium chloride dissolved in the aqueous phase. An equilibrium satisfying this condition will be a local maximum. This value is in equilibrium, but any infinitesimally small perturbations will drive the particle to a lower free energy state.

Since there is a finite amount of salt in a fixed dry diameter particle that can dissolve, the problem also has extreme bounding values that may represent stable states at

$$x_{\text{NaCl}} = 0 \quad (15)$$

and at

$$x_{\text{NaCl}} = 1. \quad (16)$$

The stable configuration is the one with the lowest free energy even if it is a bounding point.

The hygroscopic growth factor predicted for subsaturated relative humidity by the coated and uncoated (“prompt”) models show significant differences. Figure 4 illustrates the prompt deliquescence of the uncoated model and the multiple-equilibria region of the coated model. Both models predict two equilibria between deliquescence and ef-

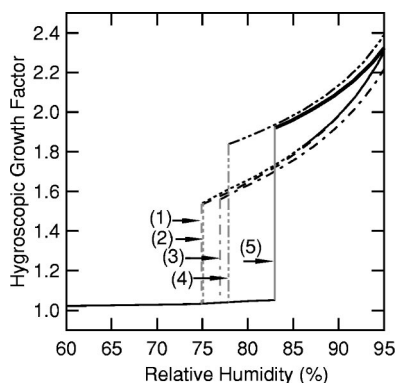


FIG. 5. Predicted hygroscopic growth curves with uncoated and coated models. For the uncoated particle model curves are shown for four sets of solution properties: (1) ideal solution, constant molar partial volume \bar{v} , and $\sigma^{\text{LV}} = 70 \text{ mN m}^{-1}$ (dashed line), (2) ideal solution, measured \bar{v} , and $\sigma^{\text{LV}} = 70 \text{ mN m}^{-1}$ (dotted line), (3) ideal solution, measured \bar{v} , and $\sigma^{\text{LV}} = 83 \text{ mN m}^{-1}$ (dashed-dotted line), (4) real solution, constant \bar{v} , and $\sigma^{\text{LV}} = 70 \text{ mN m}^{-1}$ (dashed-dotted-dotted line). For the coated model, one curve is shown for (5) real solution, measured \bar{v} , and $\sigma^{\text{LV}} = 83 \text{ mN m}^{-1}$ (solid line). The gray lines represent deliquescence. The unstable equilibria for the coated model are not shown.

fluorescence, namely for relative humidities below 75%, where the upper wet branch is metastable with respect to the dry branch in this region.² However, the coated model predicts a three-equilibria region between 80 and 87%, prompting the question of which equilibrium is the stable one. Figure 5 shows the effect of different model assumptions for the dry model on the predicted hygroscopic growth.

At constant relative humidity, the stability of each equilibrium is determined by the second derivative of the free energy surface with respect to either a constant mole fraction of dissolved NaCl, x_{NaCl} , or a constant mass ratio of condensed water

$$r_w \equiv \frac{m_w}{m_{\text{NaCl}}}, \quad (17)$$

where m_w is the mass of condensed water and m_{NaCl} is the mass of sodium chloride. Figure 6 shows examples of the free energy surface for the equilibria of the hygroscopic growth factor behavior at relative humidities of 73% and 75% (in the two-equilibrium region), 81, 83, and 85% (in the three-equilibrium region), and 90% (in the more humid two-equilibria region). To facilitate interpretation of these three-dimensional surfaces, Fig. 7 illustrates a two-dimensional slice through the free-energy minimum trough of each surface plotted against the mole fraction of dissolved NaCl, x_{NaCl} . In the two-equilibria region below 80%, the dry equilibrium is more stable than the wet. In the three-equilibria region, the dry equilibrium continues to have the minimum free energy from 80 to 83%. The difference is that a third unstable equilibrium exists where the free energy goes through a maximum value that corresponds to the equilibrium for the partially wet particle. Since this value is a maximum the equilibrium is clearly unstable, so the stable value is given by one of the extreme endpoints; at 81% relative humidity the dry branch has the lower free energy and will be stable. At 83% relative humidity, the dry and wet particles

have equal free energy, so deliquescence occurs. Above this relative humidity, the most stable equilibrium continues to be the wet branch, and this continues into the higher humidity two-equilibria region above 87%.

This transition from dry to wet equilibrium is summarized in Fig. 8, in which the free energies of the dry, wet and deliquescence branches are shown. The dry branch has the lowest free energy up to 83% relative humidity when it is crossed by the wet branch in the coated model. The uncoated model has a substantially higher dry free energy because of the high solid/vapor surface tension, resulting in intersecting the wet branch at a lower relative humidity. This model (with an appropriate solid/vapor surface tension and without idealizations) predicts the transition from dry to wet at 78%.

V. DEPENDENCE OF DELIQUESCENCE RELATIVE HUMIDITY ON PARTICLE SIZE

To illustrate the consequences of this behavior for deliquescence and hygroscopic growth of small particles, Figs. 9 and 10 show, respectively, the free energies and growth factors of particles between 8 and 100 nm dry diameter. At 100 nm, the deliquescence relative humidity of NaCl particles is negligibly different from the bulk value at 75%. The increase in deliquescence relative humidity with size decreasing from 100 to 15 nm is 8% from the initial 75 to 83% relative humidity. For a 5 nm particle, the deliquescence relative humidity increases further to 84%. However, note that at this size the adsorption of three monolayers is predicted before reaching 80% relative humidity, already accounting for a growth factor of approximately 1.2.

For smaller particles and lower growth factors, the uncertainty of the liquid surface tensions are larger, so we have estimated the uncertainty in neglecting this effect with a simple Tolman length approximation.⁶ While clearly not as accurate as more recent models of surface effects in clusters,^{22,23} Fig. 11 provides a reasonable bound on the estimated uncertainty with growth factor for these small sizes. The primary effect is that the steepness of the negative slope of the unstable equilibria is increased, although the deliquescence relative humidity changes by only 5%. In general, the higher growth factors ($GF > 1.5$) are insensitive to this problem, although just prior to disappearance of the salt crystal a similar phase ambiguity is encountered when the shrinking crystal is reduced to a finite number (< 100) of "solid" molecules. Figure 11 shows schematically the regions of the hygroscopic growth where size-dependent surface tensions may be most important, indicating regions of high uncertainty.

Figure 12 shows that a coated cubic crystal would have a 1% higher deliquescence relative humidity using an estimated surface energy approach,⁶ providing an upper bound on the uncertainty associated with crystal shape effects. The cubic crystal increases the surface tension of the crystal, but the resulting increase in the predicted deliquescence relative humidity is small compared to the coated model for a spherical crystal of equal volume.

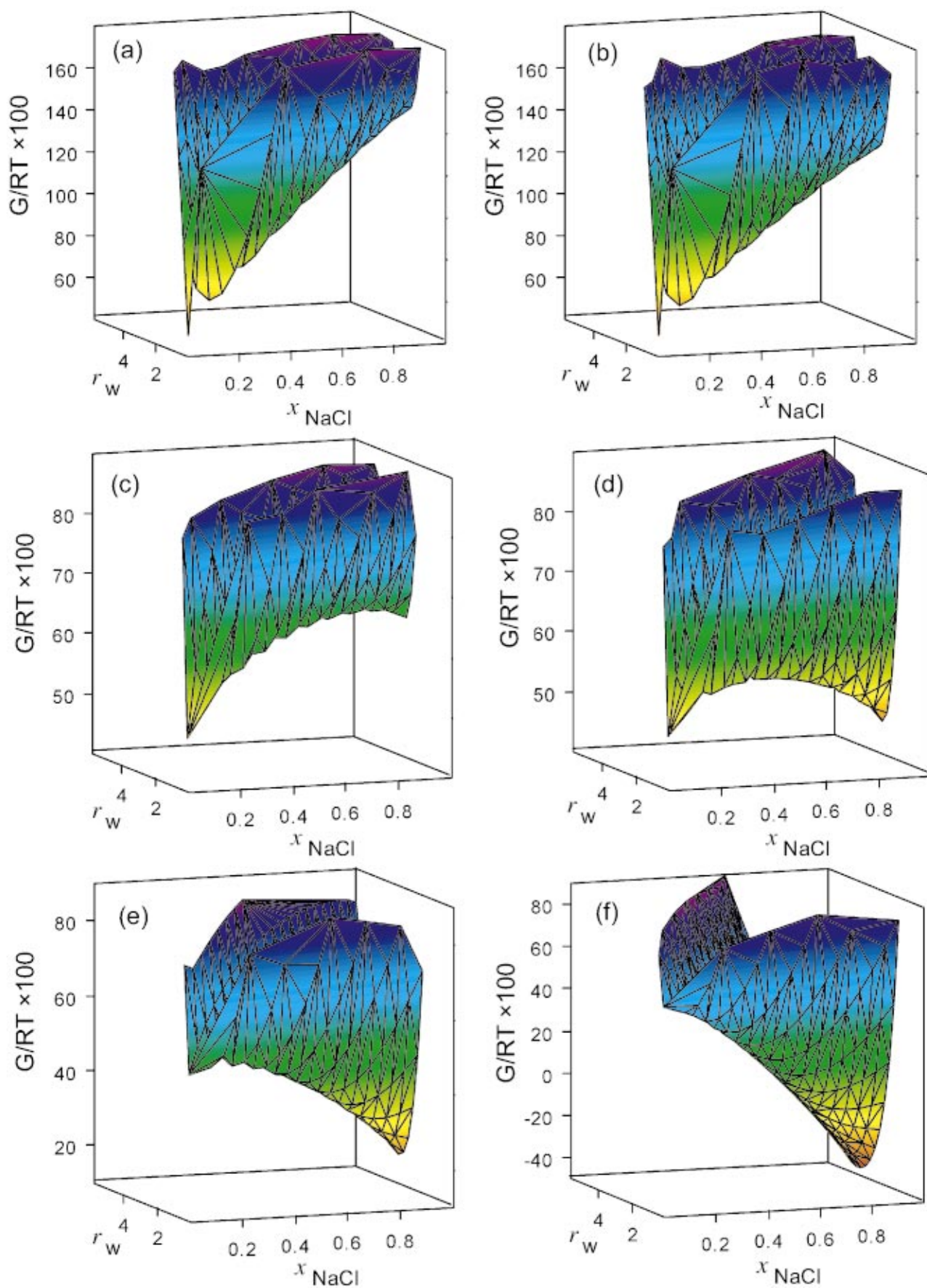


FIG. 6. (Color) Gibbs free energy surface of the coated particle model as functions of the condensed water ratio r_w and the mole fraction dissolved sodium chloride x_{NaCl} at the following relative humidities: (a) 73%, (b) 75%, (c) 81%, (d) 83%, (e) 85%, and (f) 90%.

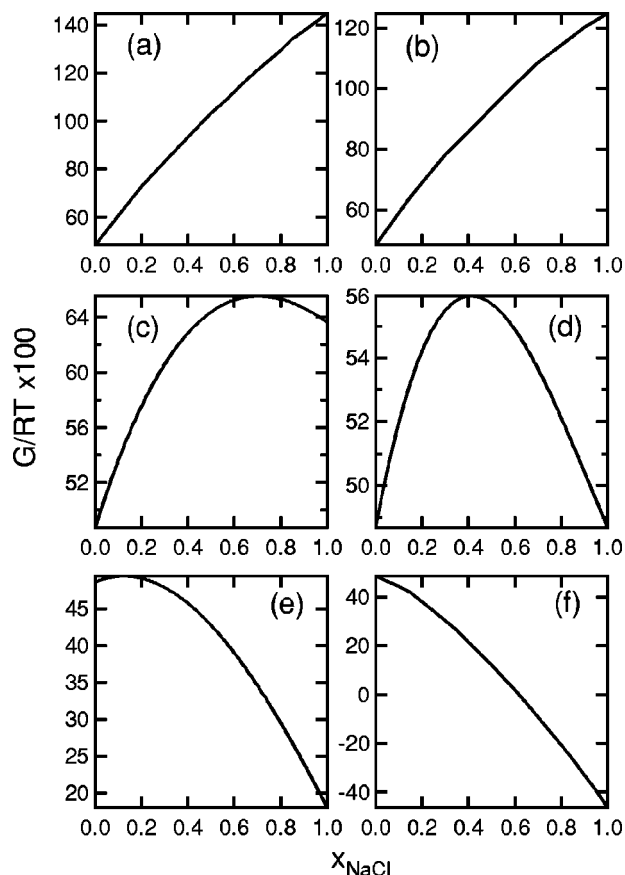


FIG. 7. Gibbs free energy of the coated particle model minimized with respect to the condensed water ratio r_w as a function of mole fraction of dissolved sodium chloride x_{NaCl} at the following relative humidities: (a) 73%, (b) 75%, (c) 81%, (d) 83%, (e) 85%, and (f) 90%. The bounding values at $x_{\text{NaCl}}=0$ and $x_{\text{NaCl}}=1$ correspond to dry and wet states, respectively. The internal maximum in (c), (d), and (e) correspond to the unstable equilibria for partially wet particles.

VI. GROWTH OF AMMONIUM SULFATE AND SOLUBLE ORGANIC PARTICLES

Both inorganic salts and organic species are expected to exhibit analogous behavior in reaching deliquescence. Exact

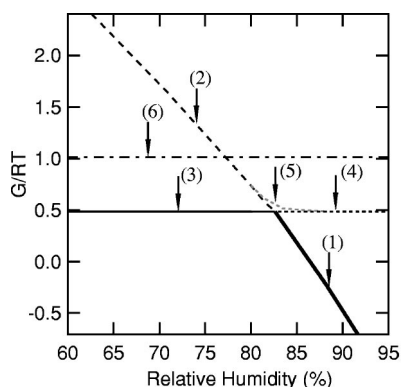


FIG. 8. Gibbs free energy of (1) stable equilibria for the wet particle (thick solid line), (2) metastable equilibria for the wet particle (dotted line), (3) stable equilibria for the dry particle (thin solid black line), (4) unstable equilibria for the dry particle (dotted line), and (5) unstable equilibria for partially wet particles (gray dotted line). The dashed-dotted line (6) represents Gibbs free energy of the dry particle in the uncoated model.

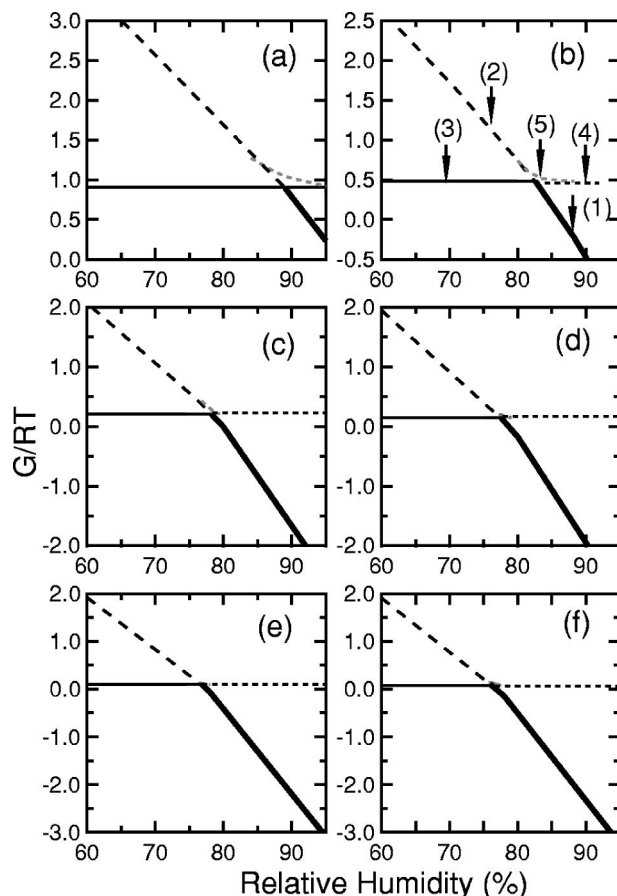


FIG. 9. Gibbs free energy of sodium chloride particles at the following dry diameters: (a) 8 nm, (b) 15 nm, (c) 35 nm, (d) 50 nm, (e) 75 nm, and (f) 100 nm. Each graph shows (1) stable equilibria for the wet particle (thick solid line), (2) metastable equilibria for the wet particle (dotted line), (3) stable equilibria for the dry particle (thin solid black line), (4) unstable equilibria for the dry particle (dotted line), and (5) unstable equilibria for partially wet particles (gray dotted line).

calculations for many species and mixtures are not possible as the needed solid/liquid, liquid/vapor, or solid/vapor surface tensions have not been measured accurately so the calculations are illustrated for a range of surface tension in Fig. 13.^{6,7} Some information is available for ammonium sulfate,^{28–31} so the predicted hygroscopic growth for 15 nm particles is illustrated in Fig. 14. The change in deliquescence point from bulk to 15 nm is similar for ammonium sulfate going from 80 to 88%. Infrared spectroscopic studies have suggested that ammonium sulfate particles may not efflorescence at relative humidities as low as 30%,^{29,30} but few measurements of water adsorption on ammonium sulfate with increasing relative humidity have been made. The coated model predictions show behavior similar to sodium chloride, although little or no water adsorption would result in behavior closer to the uncoated model.

For soluble organic compounds there are only limited data available about compound properties and deliquescence behavior,^{3,5} so in order to illustrate the behavior of lower surface tension compounds we have described a generic soluble organic compound. This compound has the molecular weight, solubility and structure of malonic acid as described by a semi-empirical model.³² Since σ^{SL} for either

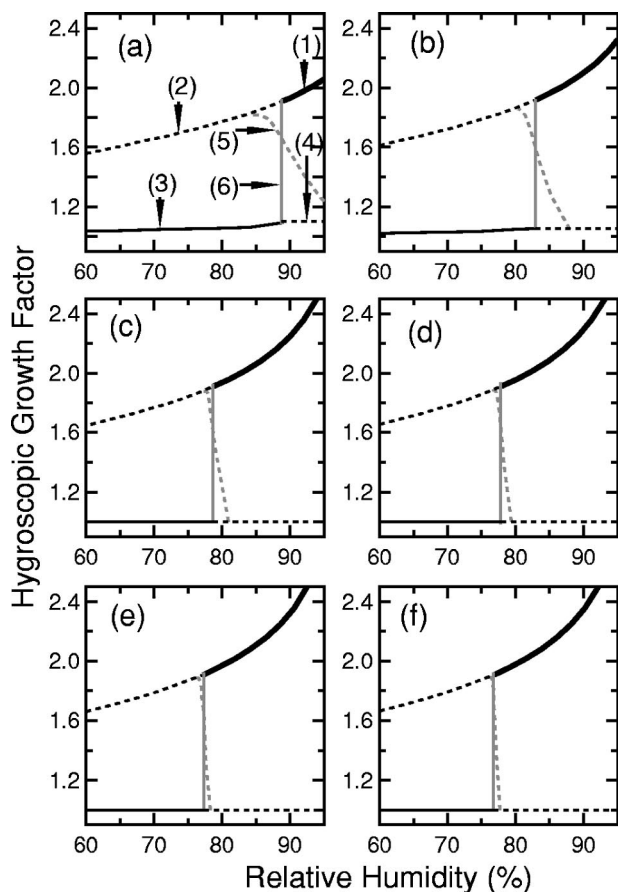


FIG. 10. Predicted hygroscopic growth curves of sodium chloride particles at the following dry diameters: (a) 8 nm, (b) 15 nm, (c) 35 nm, (d) 50 nm, (e) 75 nm, and (f) 100 nm. Each graph shows (1) stable equilibria for the wet particle (thick solid line), (2) metastable equilibria for the wet particle (dotted line), (3) stable equilibria for the dry particle (thin solid black line), (4) unstable equilibria for the dry particle (dotted line), (5) unstable equilibria for partially wet particles (gray dotted line), and (6) deliquescence (gray solid line).

malonic acid or other soluble organic compounds is not available, we have done the calculation for the range of $20\text{--}40\text{ mN m}^{-1}$, representing the low and high ends of measured solid/liquid surface tension values.⁷ The resulting soluble organic species deliquesces at a relative humidity of 76% for bulk solutions, but for 15 nm particles deliquescence occurs at 82% relative humidity for $\sigma^{SL} = 20\text{ mN m}^{-1}$ and 75% for $\sigma^{SL} = 40\text{ mN m}^{-1}$. In the latter case, the solid/liquid surface tension is sufficiently high that the deliquescence relative humidity actually decreases as the dry diameter decreases to 15 nm. This behavior is unusual since most surface tension values measured to date result in a decrease in *DRH* as predicted for inorganic salts.

In summary, for the three species studied, similar increases in deliquescence relative humidity were found, as is illustrated in Fig. 15. Between bulk behavior and 5 nm particles, sodium chloride, ammonium sulfate, and a soluble organic compound all are expected to increase between 8 and 10% in deliquescence relative humidity. This result (and the well-behaved nature of the relationship) suggests that the behavior will also hold for other water-soluble salts.

Since a large part of this phenomenon results from the

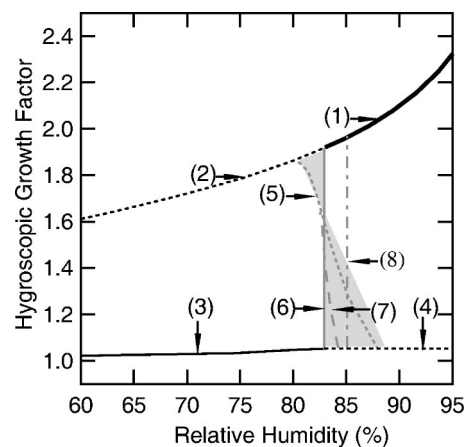


FIG. 11. Estimated error in predicted hygroscopic growth factor of 15 nm dry diameter sodium chloride particles due to size-dependent surface energy artifacts. The coated particle model is calculated with constant $\sigma^{LV} = 83\text{ mN m}^{-1}$ for (1) stable equilibria for the wet particle (thick solid line), (2) metastable equilibria for the wet particle (dotted line), (3) stable equilibria for the dry particle (thin solid black line), (4) unstable equilibria for the dry particle (dotted line), (5) unstable equilibria for partially wet particles (gray dotted line), and (6) deliquescence (gray solid line). The coated particle calculations were repeated with size-dependent surface tension from Tolman length giving identical predictions for stable branches, (7) unstable equilibria for partially wet particles (dashed gray line), and (8) deliquescence (dashed-dotted gray line). The shaded area provides a schematic indication of the relative error incurred by using bulk surface tension in the coated particle model (Ref. 6). The wet particle branch for both models is shown in the thick solid line.

Kelvin effect increasing the surface energy for forming small particles, this result is expected to be quite general. Exceptions are cases in which the surface energy of the solid/liquid interface overwhelmed the energy of the liquid/vapor interface. While some organic species have low liquid/vapor surface tensions, it seems unlikely that they have sufficiently

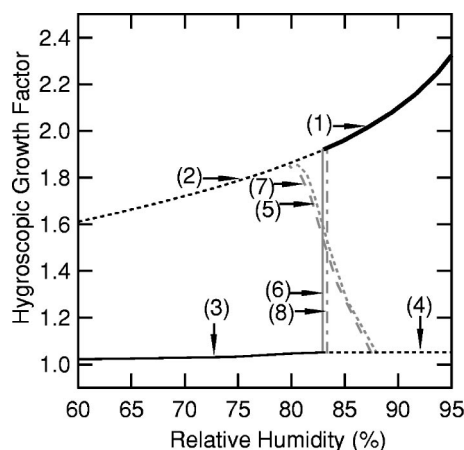


FIG. 12. Predicted hygroscopic growth factor of 15 nm dry diameter sodium chloride particles for the coated model with spherical NaCl crystals showing (1) stable equilibria for the wet particle (thick solid line), (2) metastable equilibria for the wet particle (dotted line), (3) stable equilibria for the dry particle (thin solid black line), (4) unstable equilibria for the dry particle (dotted line), (5) unstable equilibria for partially wet particles (gray dotted line), and (6) deliquescence (gray solid line). The cubic NaCl crystal assumption yields the curves shown for (7) unstable equilibria of partially wet particles (dashed gray line) and (8) deliquescence (dashed-dotted gray line).

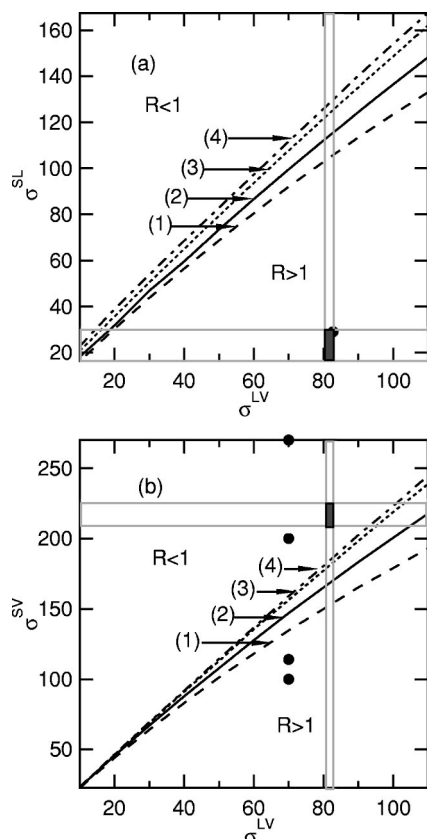


FIG. 13. Constant deliquescence relative humidity ratio isopleths at $R=1$ for ranges of solid/liquid surface tension σ^{SL} and liquid/vapor surface tension σ^{LV} for (a) the coated particle model and (b) the uncoated particle model (Refs. 7, 25, 26). Dry diameter sizes shown here are (1) 8 nm (dashed line), (2) 15 nm (solid line), (3) 35 nm (dotted line), and (4) 50 nm (dash-dotted line). The shaded area illustrates the current reported measurements of σ^{SL} , σ^{LV} , and σ^{SV} . The circles represent the values used in the uncoated model in Figs. 2, 3, and 5.

high solid/liquid surface tensions to compensate for the Kelvin effect.

An alternative scenario may arise in the atmosphere for wetting organic species or mixtures which exist in the ab-

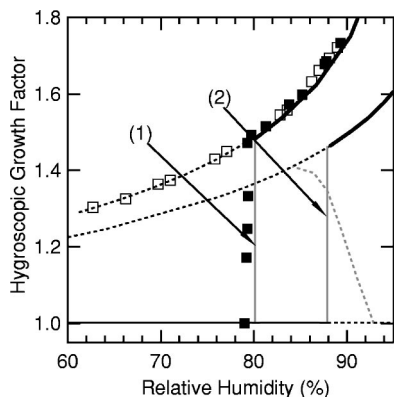


FIG. 14. Predicted hygroscopic curve of 15 nm ammonium sulfate. The thick solid black lines represents wet particles, thin solid black line dry particles, and gray solid line deliquescence. The dotted line represents metastable and unstable equilibria. For ammonium sulfate, deliquescence was calculated for (1) bulk and (2) 15 nm solutions are shown, both with $\sigma^{SL} = 29 \text{ mN m}^{-1}$. The solid squares show measured values for ammonium sulfate deliquescence in bulk solution (Ref. 28) (solid squares).

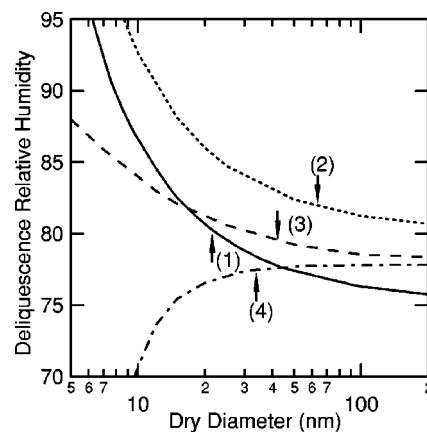


FIG. 15. Dependence of predicted deliquescence relative humidities on particle dry diameter for (1) sodium chloride (solid line), (2) ammonium sulfate (dotted line), (3) soluble organic compound with $\sigma^{SL} = 20 \text{ mN m}^{-1}$ (dashed line), and (4) soluble organic compound with $\sigma^{SL} = 40 \text{ mN m}^{-1}$. These calculations are based on the coated particle model.

sence of water as liquids rather than solids in atmospheric conditions. In this case a liquid, the nonaqueous core is surrounded by saturated water, so that the relevant interfaces are the liquid/liquid interface between the organic liquid and the aqueous solution, and then the liquid/vapor interface with air. This scenario could result in contradictory behavior, as the organic liquid may coat the aqueous phase rather than vice versa.³

VII. INTERPRETATION OF MEASUREMENTS

Recent work by Hämeri *et al.*⁴ provides a preliminary opportunity to compare with measurements of this phenomenon. Their data show deliquescence relative humidities of 83 ± 2 and $87 \pm 2\%$ for dry diameters of 15 and 8 nm in ammonium sulfate particles, illustrating the same trend as the predicted values of 81 ± 3 and $83 \pm 3\%$, both shown in Fig. 16. However, they measured a few data points intermediate to the dry and wet states that occur in the range that the coated model predicts to represent only unstable equilibria. One possible explanation is that the residence time for humidification between the two differential mobility analyzers was insufficient to reach equilibrium with the water vapor. The measured data points might then represent transient values for incompletely grown particles rather than equilibria. Long residence times required for some water vapor equilibria have been noted by investigators with time-varying observing techniques for larger particles.²

Another possibility is that these small ammonium sulfate particles were contaminated by organic species during particle production and analysis. The authors report contamination of less than 1% of the ammonium sulfate bulk solution, but it is possible that a surface-active contaminant may have been concentrated by the particle formation process as has been observed in other systems.^{33,34} This type of enhancement of surface-active agents will be greater in smaller particles, since the surface-to-volume ratio is higher. To understand the role that contamination may have played in these measurements of ammonium sulfate particles, we have shown in Fig. 16 the hygroscopic growth for ammonium

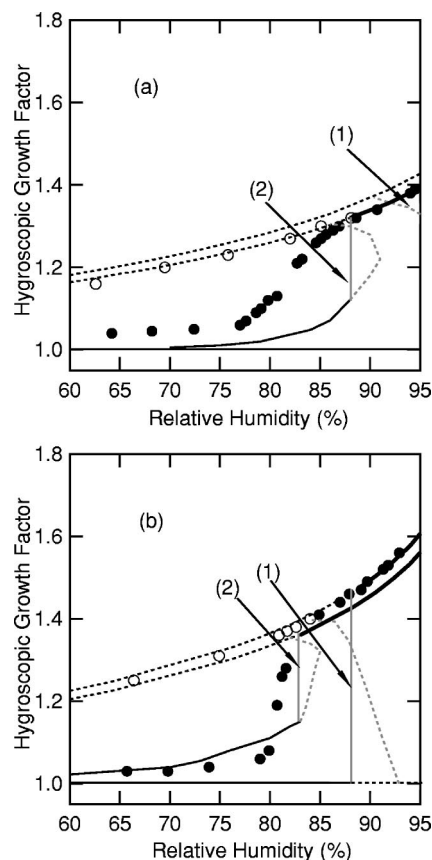


FIG. 16. Comparison of predicted hygroscopic growth curves with measurements from Hämeri *et al.* (Ref. 4) for deliquescence (solid circles) and efflorescence (empty circles) for two dry diameters: (a) 8 and (b) 15 nm. In both panels, thick solid black lines represent wet particles, thin solid black lines dry particles, and gray solid lines deliquescence. All dotted lines represent metastable and unstable equilibria. Both panels show deliquescence calculated from the coated particle model for (1) 100% ammonium sulfate and (2) 90% ammonium sulfate with 10% malonic acid.

sulfate with 1 and 10% organic contaminant, where we have used malonic acid to represent the solution properties of a typical organic contaminant and a semi-empirical model for the organic-electrolyte interactions in aqueous solution.^{32,35} While a 1% organic mixture shows behavior similar in slope to that observed, it is not sufficient to account for the early growth measured. A mixture of ammonium sulfate with 10% malonic acid represents a reasonable approximation of the deliquescence slope, and also matches the measured data better after deliquescence.

Resolving this discrepancy from experiment may be possible. To check if the particles in the deliquescing region have reached stability, it would be possible to add a humidity-controlled flow tube with an increased residence time. If the results vary with residence time, the measured points clearly do not represent stable equilibria. Variation in the relative humidity in the flow tube will also need to be eschewed to preclude anomalous results. Resolving the issue of contamination may be more difficult, since removing trace organic impurities even in clean laboratory conditions is problematic. Alternatively the composition of organic species in 15 nm particles could be measured, but since this composition measurement is currently not practical in this

size range, it may be difficult to establish the purity of the particles produced.

Despite these uncertainties, hygroscopic growth experiments are capable of measuring stable (and sometimes metastable) equilibria formed when small particles deliquesce. Additional experiments might be able to not only confirm the increase in deliquescence relative humidity with decreasing particle size (even though they are unable to measure transient states in the deliquescing region), but also to allow size-dependent surface tension measurements. For example, by measuring the deliquescence relative humidity of particles as small as 3 nm, the effective surface tension can be calculated as a function of particle size.

VIII. CONCLUSIONS

A model of the deliquescence of coated particles smaller than 100 nm diameter based on accurate chemical and physical properties predicts that the deliquescence relative humidity will increase as particle size is decreased for sodium chloride and ammonium sulfate. This approach relies on bulk surface tension values but the trend is independent of the exact values chosen. The result is dependent on the shape of the dry particle and assumes that the particle will have adsorbed water on its surface. Current data support these assumptions for a range of soluble atmospheric constituents and their mixtures, including sodium chloride and ammonium sulfate.

While the increase in deliquescence point with decreasing particle size is consistent in the systems studied, a dearth of data for the behavior of interfaces for sulfate salts and organic species results in increased uncertainties in those predictions. Hygroscopic growth measurements of ammonium sulfate particles taken by another group⁴ are consistent with the predicted deliquescence relative humidities for 8 and 15 nm particles, but data taken in the deliquescence region cannot be explained. Additional experiments are suggested that not only may be able to resolve these discrepancies but also may be able to provide a means to measure the size-dependent surface tension of particles as small as 3 nm dry diameter with current techniques.

ACKNOWLEDGMENTS

This work was supported by the National Science Foundation under Grant No. ATM-9732949. The authors also acknowledge a helpful discussion with P. G. Debenedetti who generously agreed to review Y.M.'s graduate research and suggested an analytical approach to part of this problem complementary to the computational models we have compared here.

¹P. J. Adams, J. H. Seinfeld, D. Koch, L. Mickley, and D. Jacob, *J. Geophys. Res.* **106**, 1097 (2001).

²I. N. Tang, H. R. Munkelwitz, and N. Wang, *J. Colloid Interface Sci.* **114**, 409 (1986).

³C. N. Cruz and S. N. Pandis, *Environ. Sci. Technol.* **34**, 4313 (2000).

⁴K. Hämeri, M. Väkevää, H.-C. Hansson, and A. Laaksonen, *J. Geophys. Res.* **105**, 22231 (2000).

⁵A. J. Prenni, P. J. DeMott, S. M. Kreidenweis, D. E. Sherman, L. M.

- Russell, and Y. Ming, *J. Phys. Chem.* (submitted).
- ⁶R. Defay, I. Prigogine, and A. Bellemans, *Surface Tension and Adsorption* (Longmans Green, London, 1966).
- ⁷A. W. Adamson, *Physical Chemistry of Surfaces* (Wiley, New York, 1990).
- ⁸H. T. Davis, *Statistical Mechanics of Phases, Interfaces, and Thin Films* (VCH Publishers, New York, 1995).
- ⁹P. Mirabel, H. Reiss, and R. K. Bowles, *J. Chem. Phys.* **113**, 8200 (2000).
- ¹⁰R. A. Lad, *Surf. Sci.* **12**, 37 (1968).
- ¹¹P. B. Barraclough and P. G. Hall, *Surf. Sci.* **46**, 393 (1974).
- ¹²J. Estel, H. Hoinkes, H. Kaarmann, H. Nahr, and H. Wilsch, *Surf. Sci.* **54**, 393 (1976).
- ¹³S. Ghosal and J. C. Hemminger, *J. Phys. Chem. A* **103**, 4777 (1999).
- ¹⁴B. J. Finlayson-Pitts and J. C. Hemminger, *J. Phys. Chem. A* **104**, 11463 (2000).
- ¹⁵D. D. Weis and G. E. Ewing, *J. Geophys. Res.* **104**, 21275 (1999).
- ¹⁶Z. L. Wang, J. M. Petroski, T. C. Green, and M. A. El-Sayed, *J. Phys. Chem. B* **102**, 6145 (1998).
- ¹⁷S. J. Peters and G. E. Ewing, *Langmuir* **13**, 6345 (1997).
- ¹⁸S. J. Peters and G. E. Ewing, *J. Phys. Chem. B* **101**, 10880 (1997).
- ¹⁹M. Foster and G. E. Ewing, *Surf. Sci.* **427–428**, 102 (1999).
- ²⁰M. C. Foster and G. E. Ewing, *J. Chem. Phys.* **112**, 6817 (2000).
- ²¹W. F. Espenschied, E. Matijevic, and M. Kerker, *J. Phys. Chem.* **68**, 2831 (1964).
- ²²S. L. Girshick and C.-P. Chiu, *J. Chem. Phys.* **93**, 1273 (1990).
- ²³G. Wilemski, *J. Chem. Phys.* **103**, 1119 (1995).
- ²⁴L. R. Fisher and J. N. Israelachvili, *Nature (London)* **277**, 548 (1979).
- ²⁵A. A. Abramzon and R. D. Gauberk, *Zh. Prikl. Khim. (St. Petersburg)* **66**, 1428 (1993).
- ²⁶W. Wu and G. H. Nancollas, *Adv. Colloid Interface Sci.* **79**, 229 (1999).
- ²⁷H. C. Allen, M. L. Mecartney, and J. C. Hemminger, *Microsc. Microanal.* **4**, 23 (1998).
- ²⁸I. N. Tang and H. R. Munkelwitz, *Atmos. Environ.* **27**, 467 (1994).
- ²⁹I. N. Tang, K. H. Fung, D. G. Imre, and H. R. Munkelwitz, *Aerosol. Sci. Technol.* **23**, 443 (1995).
- ³⁰D. D. Weis and G. E. Ewing, *J. Geophys. Res.* **101**, 18709 (1996).
- ³¹H. R. Pruppacher and J. D. Klett, *Microphysics of Clouds and Precipitation* (Kluwer Academic, Norwell, MA, 1997).
- ³²Y. Ming and L. M. Russell, *AIChE J.* (submitted).
- ³³D. C. Blanchard and L. Syzdek, *Science* **170**, 626 (1970).
- ³⁴J. A. Quinn, R. A. Steinbrook, and J. L. Anderson, *Chem. Eng. Sci.* **30**, 1177 (1975).
- ³⁵Y. Ming and L. M. Russell, *J. Geophys. Res.* (in press).